Chapter 5

Evaluation of the New Phi-Plot Modeling Approach Optimization by Stepwise Solvent Gradient Simulated Moving Bed (SG-SMB) Simulator

Leôncio Diógenes Tavares Câmara

Additional information is available at the end of the chapter

http://dx.doi.org/10.5772/61252

Abstract

A new analytical design approach for operating conditions determination of solvent gradient simulated moving bed (SG-SMB) processes was proposed, which was based on the equilibrium theory. Also a new implemented simulator for SG-SMB was proposed to evaluate the new design approach. The simulator was totally developed in FORTRAN 90/95, assuming a stepwise modeling approach with a lumped mass transfer model between the solid adsorbent and liquid phase. The influence of the solvent modifier was considered by applying the Abel model, which takes into account the effect of modifier volume fraction over the partition coefficient. The optimal conditions determined from the new design approach were compared to the simulation results of a SG-SMB unit applied to the experimental separation of the amino acids phenylalanine and tryptophan. The new design approach, which is based on χ equation and phi-plot analysis, was able to predict a great number of operating conditions for complete separation of such molecules, which was validated by the simulations carried out by the new SG-SMB simulator. Such a SG-SMB simulator provides simulation results with very good agreement fitting the experimental data of the amino acid concentrations both in the extract as well as in the raffinate.

Keywords: Simulated moving bed, modeling, optimization

1. Introduction

The simulated moving bed (SMB) process has been used successfully in the separation of all kinds of molecules. It is a continuous process of interconnected chromatographic columns (HPLC), which can be used to separate molecule mixtures (enantiomeric and nonenantiomeric) with high purity and low solvent consumption. In the process, the positions of the two inlet

(feed and solvent) and the two outlet (extract and raffinate) streams are changed in the clockwise direction, leading to a simulated countercurrent movement of solid adsorbent phase. The extract and raffinate streams collect the more and less adsorbable enantiomer molecules, respectively. The solvent strength in the solvent gradient simulated moving bed (SG-SMB) process is modulated along the sections as the volume fraction of the modifier (ϕ) can be altered as can be seen in Fig. 1. The introduction of ethanol (modifier) in the desorbent stream leads to higher values of the modifier volume fraction at sections I and II, which reduces the adsorption affinity of the molecules in these regions. The contrary is observed in sections III and IV as the absence of ethanol in the inlet feed stream reduces the volume fraction of modifier in these regions, which consequently increase the adsorption affinity of molecules. Such procedures usually increase the purity of products as well as the productivity, reducing solvent consumption.

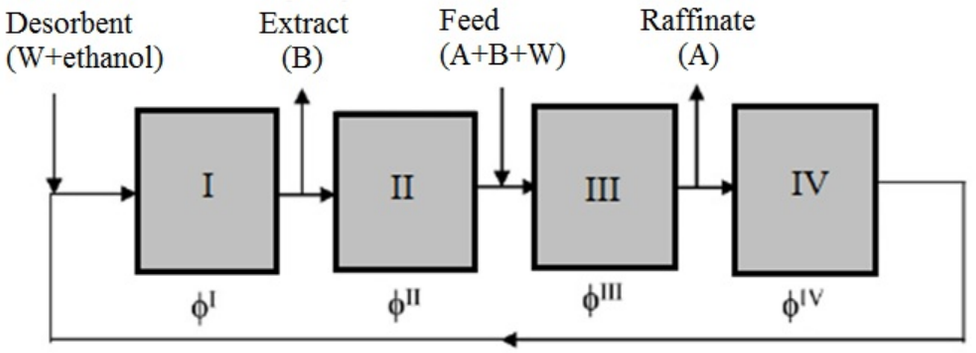

Figure 1. Schematic representation of SG-SMB

The application of gradients can be used in the performance improvement of simulated moving bed (SMB) as well as true moving bed (TMB) chromatography in which the most usual is the solvent-gradient method applied to SMB processes [1-15]. Other techniques include temperature gradients in SMB [16], micellar gradients in size-exclusion SMB [17], salt gradients in size-exchange SMB [18], pressure gradient in supercritical eluent SMB [19], voltage gradients in true moving bed (TMB) electrophoresis [20], etc. Migliorini et al. [16] showed the feasibility of temperature gradients applied in SMB, which may lead to significant advantages over the isothermal process mode. The authors observed an improvement in the productivity and a remarkable reduction in the solvent consumption with the possibility of tuning the enrichment by selection of proper temperature profile. Horneman et al. [17] showed the viability of surfactant-aided size-exclusion chromatography (SASEC) application on a SMB unit through selectivity modification by the addition of non-ionic micelles to the mobile phase. The use of a correct gradient leads to a significantly higher throughput of product concentration, which also leads to a lower solvent consumption if compared to a conventional SEC-SMB.

In the most common solvent-gradient simulated (SG-SMB) process as well as in other SMB gradient techniques, the main objective is the determination of flow rates and switching time, which leads to the full separation of molecules (high purity) with great productivity and low solvent consumption. Such a challenging objective can be achieved by utilizing, in general,

http://dx.doi.org/10.5772/61252

either inverse problem optimization routines [1-4] or design criteria [5-8]. The application of inverse routines coupled with adequate mathematical mass transfer models [1-4] of the chromatographic column representations is desirable in the optimization problems for the achievement of optimal operating conditions. The inverse routine approach is interesting in the SG-SMB process optimization field as it can incorporate more realistic phenomenon effects such as mass transfer resistance, finite column efficiency, purity constrains, etc. The main disadvantages of such approaches are related to the high computational cost due to numerical simulations and to the algorithm accuracy and efficiency in the search for optimal solutions. The work of Nam et al. [1] is a good example as the authors utilized an inverse routine (based on genetic algorithm) combined with detailed mass transfer chromatographic rate models in the optimization of SG-SMB separation of phenylalanine and tryptophan. The optimization routine in this case was able to determine successfully the best operating conditions, which were further utilized and confirmed experimentally through a SG-SMB unit. The utilization of design criteria [5-8] is important in the determination of regions of complete separation. The design criteria approach is based on the frame of chromatography equilibrium theory or the so-called triangle theory in which the axial dispersion as well as the mass transfer resistance are neglected. Moreover, it is assumed that the separation performance of SG-TMB and SG-SMB is the same, and neither the main solvent nor the modifier interacts with the adsorbent phase. Abel et al. [7,8] provided design criteria and optimization results for the cases of linear and Langmuir isotherms, respectively. The authors carried out simulations from a mathematical mass transfer model with overall mass transfer and axial dispersion coefficients to confirm the validity of the theoretical analysis. In the work of Antos and Seidel-Morgenstern [5], a design criteria strategy, also based on the triangle theory, was coupled to mass transfer models (mixed cells in series) in the determination, through systematic numerical calculations, of suitable operating conditions as a function of averaged desorbent concentrations. The publication of Mazzotti et al. [19] in 1997 is maybe the first one in the literature which extends the isocratic concepts of the triangle theory to study and optimize a SMB gradient process or more specifically the pressure gradient mode in supercritical fluid SMB (SF-SMB).

The relevance and importance of the concepts of the triangle theory to study and evaluate the design criteria of solvent-gradient SMB (SG-SMB) processes were the motivation to proceed in the same direction applying such theory to establish a general project equation (χ equation) for optimal operating condition determination. The first step in such development, which was published recently [9] in a previous study (part I) showed the potential of the proposed screening strategy. It was used as the basis for further and deep studies for the present work (part II) in the analysis and evaluation of different operating conditions for performance improvement related to the separation of the amino acids phenylalanine and tryptophan. The proposed screening strategy was not used as usually described in the literature in the determination of regions of complete separation, but it was used in the minimization of the gradient of χ equation with the analysis of modifier volume fraction (Phi-plot) to determine the viability of separation (high purity in the extract and raffinate). A new implemented simulator for SG-SMB was also proposed to evaluate the new design approach, which assumed a stepwise modeling approach with a lumped mass transfer model between the solid adsorbent and liquid phase.

2. Phi-plot design criteria

Mazzotti et al. [4] proposed an approach, which is considered the classical procedure in the determination of the operating conditions of isocratic SMB process. The classical approach of Mazzotti et al. [4] was extended analogously to solvent gradient conditions (SG-SMB) considering the Henry's constant a function of the modifier volume fraction.

$$\mathbf{H}_{(+)}(\phi) < \mathbf{m}_{\mathrm{I}} < \infty \tag{1}$$

$$\mathbf{H}_{(-)}(\phi) < \mathbf{m}_{\mathrm{II}} < \mathbf{H}_{(+)}(\phi) \tag{2}$$

$$\mathbf{H}_{(-)}(\phi) < \mathbf{m}_{\mathrm{III}} < \mathbf{H}_{(+)}(\phi) \tag{3}$$

$$\frac{-\varepsilon_p}{(1-\varepsilon_p)} < \mathbf{m}_{\mathrm{IV}} < \mathbf{H}_{(-)}(\phi) \tag{4}$$

in which ε_p, m_i, $H_{(+)}$, and $H_{(-)}$ correspond to intraparticle porosity, flow rate ratios in each section i, and the Henry constants for the more and less adsorbable molecules, respectively.

Fig. 2A shows a typical volume fraction distribution of modifier along columns, assuming the introduction of modifier only in the desorbent inlet stream. As can be seen in Fig. 2A the modifier volume fraction reduces drastically in the forward positions after the feed inlet stream. Such a modifier volume fraction profile can be achieved assuming or not the adsorption of modifier by solid adsorbent phase. The results of Fig. 2A were obtained carrying out simulations through the proposed stepwise modeling of SG-SMB, which is described in the next section. In the proposed SG-SMB stepwise modeling approach the modifier adsorption by the adsorbent phase was not considered, and only the convection of ethanol (modifier) by a stepwise procedure (mixed cells in series) was assumed. In the work of Mun et al. [2], similar results of volume fraction of modifier along the columns were observed for the same condition of modifier introduction only in the desorbent inlet stream. The results are similar, but it should be noted that the authors assumed various phenomena for the ethanol (modifier) as convection, dispersion, film mass-transfer, intra-particle diffusion, and adsorption in a robust chromatographic mass transfer rate model. An important property in the design criteria is the average modifier volume fraction ($\hat{\phi}$), which is obtained from the arithmetic mean between the volume fraction of modifier in sections II (ϕ_{II}) and III (ϕ_{III}).

$$\hat{\phi} = \frac{\phi_{II} + \phi_{III}}{2} \tag{5}$$

http://dx.doi.org/10.5772/61252

The volume fraction of modifier in section II (ϕ_{II}) is equal to the volume fraction in the desorbent inlet stream (ϕ_0), and ϕ_{III} is obtained from the flow rate balance in the feed node (SG-SMB open loop case)

$$\phi_{III} = \frac{(F_D - F_E)\phi_0}{(F_D - F_E + F_F)} \tag{6}$$

in which F_D, F_E, and F_F correspond to flow rate of desorbent, extract and feed, respectively.

The Henry values can be calculated according to volume fraction of modifier along the columns (Fig. 2A), and they can be plotted along the sections II and III as difference in terms of the inequalities of Eqs. 2 and 3 leading to the inversion of the profiles (Fig. 2B).

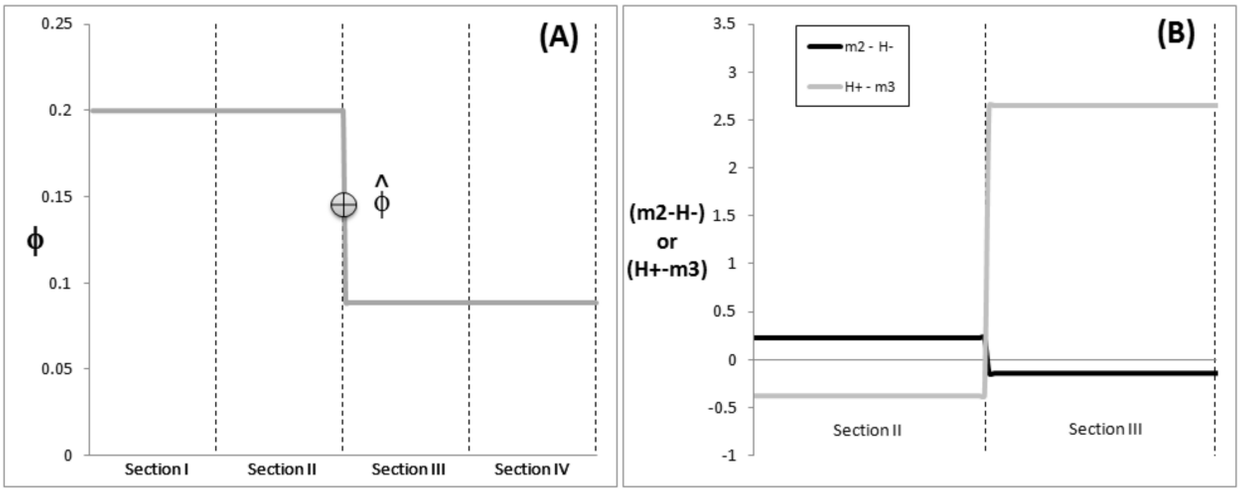

Figure 2. Modifier volume fraction along the sections (A); Inversion in the flow rates ratio difference near the feed inlet (B)

The inversion in the profiles of the difference (flow rate and Henry) along sections II and III is desirable, since for complete separation of the molecules the inequalities should be as follows:

$$\mathbf{m}_{\mathrm{II}} > \mathbf{H}_{(-)}(\phi_{\mathrm{II}}) \text{ and } \mathbf{H}_{(+)}(\phi_{\mathrm{III}}) > \mathbf{m}_{\mathrm{III}} \tag{7}$$

or

$$\mathbf{m}_{\mathrm{II}} - \mathbf{H}_{(-)}(\phi_{\mathrm{II}}) > 0 \text{ and } \mathbf{H}_{(+)}(\phi_{\mathrm{III}}) - \mathbf{m}_{\mathrm{III}} > 0 \tag{8}$$

At the feed entrance (limits of sections II and III), there is an intersection in the flow rate-Henry difference profiles so the above inequalities (Eq. 8) can be combined as

$$\mathbf{H}_{(+)}\left(\hat{\phi}\right)+\mathbf{H}_{(-)}\left(\hat{\phi}\right)=\mathbf{m}_{\mathrm{II}}+\mathbf{m}_{\mathrm{III}} \tag{9}$$

in which the Henry values for the more adsorbed molecules, $\mathbf{H}_{(+)}(\hat{\phi})$, and the less adsorbed molecules, $\mathbf{H}_{(-)}(\hat{\phi})$, are functions of the average volume fraction of modifier. The Eq. (9) is described as the difference of the terms leading to the project design equation (χ equation)

$$\chi=\mathbf{H}_{(+)}\left(\hat{\phi}\right)+\mathbf{H}_{(-)}\left(\hat{\phi}\right)-\mathbf{m}_{\mathrm{II}}+\mathbf{m}_{\mathrm{III}} \tag{10}$$

From Eq. (10) it can be noted that the best operating condition corresponds to that in which terms difference tends to zero ($\chi \to 0$).

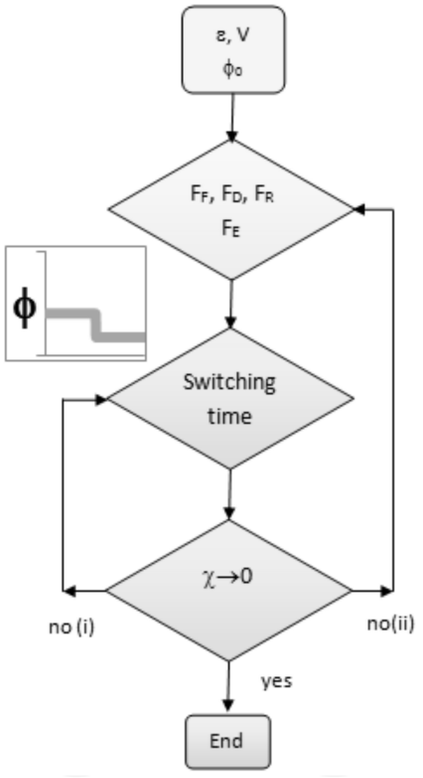

Figure 3. Flowchart of χ-equation design procedure

The flowchart of Fig. 3 describes the optimization routine, which starts with the specification of chromatographic columns volume, total porosity, and volume fraction of modifier at desorbent (ϕ_0). The next step is the specification of the volumetric flow rates followed by the switching time, which is the first one that can be varied to achieve the optimum condition of Eq. 10 ($\chi \to 0$). Both the switching time (way no (i)) as well as the volumetric flow rates (way no (ii)) can be varied in order to minimize the difference of terms in Eq. 10 ($\chi \to 0$). The evaluation of Eq. 10 is carried out analyzing at the same time the plot of the flow rate–Henry

http://dx.doi.org/10.5772/61252

differences according to volume fraction of modifier (phi-plot). For complete separation of molecules (more and less adsorbable) it is necessary to locate both curves (one for each kind) in the positive region of the phi-plot graph. The proposed optimization routine can be implemented easily as an excel spreadsheet in such way that the user can alter manually the SG-SMB conditions and at the same time evaluate the separation performance.

3. Modeling approach of SG-SMB simulator

The chromatographic columns of the SG-SMB process are modeled as a discrete representation of *N* mixed cells in series [21]:

$$\frac{dC_i^p}{dt} + \frac{dq_i^p}{dt} = (C_{i0}^p - C_i^p)\sigma_i^p \tag{11}$$

In which $\mathbf{q_i^p}$, $\mathbf{C_i^p}$, $\mathbf{C_{i0}^p}$, and t represent the compound i concentration in the solid adsorbent phase, the compound i concentration in the liquid phase, the compound i concentration in the liquid phase at the mixed cell entrance, and the time, respectively, all at column p. In Eq. 11, $\boldsymbol{\sigma_i^p = F / V}$ with V, F, and ε representing the volume, the volumetric flow rate, and the total porosity of the mixed cell, respectively. In the Eq. 11 it is assumed that the molecules in the mass transfer between the liquid and solid phase stays at the interface inside the liquid phase so the same liquid volume is used in the calculation of concentrations. Therefore, the retention factor, *ki*, is equal to the equilibrium constant, *Keq*, since the volume is the same for the liquid and solid concentrations.

In such a modeling approach the ethanol adsorption on the solid adsorbent phase was not considered, so in the mass balance of modifier (Eq. 12) along the chromatographic column, the same stepwise model for the ethanol convection along chromatographic columns without the mass transfer resistance term was assumed.

$$\frac{d\phi^p}{dt} = (\phi_0^p - \phi^p)\sigma_i^p \tag{12}$$

In Eq. 11, a lumped mass transfer model representing all the effects of mass transfer between the liquid and the solid adsorbent phase is assumed. The isotherms were utilized only in the mass transfer parameters determination in the chromatographic column characterization step. Therefore, the slow mass transfer kinetic is the main and dominant effect of mass transfer between the phases (solid and liquid). The lumped mass transfer kinetic model is presented in Eq. 13, below, which depends on the concentrations as well as the mass transfer kinetic parameters of adsorption (η_{1i}) and desorption (λ_{2i}).

$$\frac{dq_i^p}{dt} = \eta_{1i} C_i^p - \lambda_{2i} q_i^p \tag{13}$$

The solute mass balances at the nodes of the SG-SMB process of Fig. 1 is solved incorporating the volumetric flow rates of each stream (Feed, Desorbent, Extract, and Raffinate). The new mass balance of solutes at the nodes is recalculated after each change in the configuration of the streams to be incorporated into the global mass balance equations of the columns. The Eqs. 11 to 13 are organized explicitly according to a simple finite difference approach and solved numerically utilizing a 4th order Runge-Kutta method, with a time step equal to 10^{-4}, utilizing Fortran90/95.

4. Results and discussions

4.1. Column characterization by SG-SMB simulator

The column characterization is the first step in the implementation of the SG-SMB simulator. The adapted experimental results of Nam et al. [22] in Fig. 4 show that the peak residence time of phenylalanine and tryptophan is a function of the volume fraction of modifier (ϕ). In such experimental results it can be observed reduction in the affinity of solutes with the adsorbent phase, increasing the volume fraction of adsorbent (ϕ), which reduces the elution time or residence time of molecules. As can be seen in Fig. 4, tryptophan (Fig. 4B) is the more adsorbed molecule due to higher values of residence time of the molecules in the chromatographic columns.

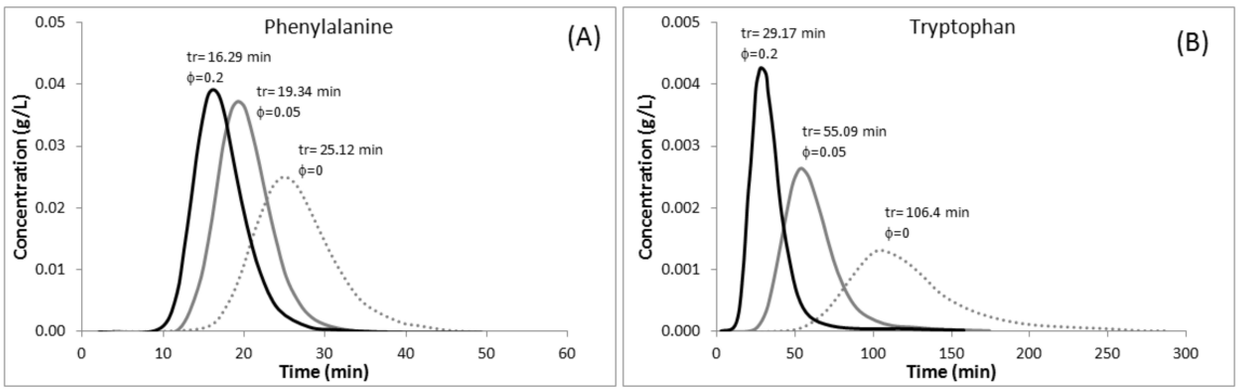

Figure 4. Adapted experimental results of Nam et al.[22]

The residence times of the two kinds of molecules (phenylalanine and tryptophan) in Fig. 4 were utilized in the column characterization for the determination of the mass transfer parameters of the lumped mass transfer model (Eq. 13). For each amino acid, in each condition of the volume fraction of modifier (ϕ=0, 0.05 and 0.2), it was determined the mass transfer parameters of adsorption and desorption that led to the same experimental value of residence

http://dx.doi.org/10.5772/61252

time. In such procedures, an important property utilized was the partition coefficient (K), which was obtained by the Abel's model [1, 23]

$$\mathbf{K} = \frac{\mathbf{p}_1}{(1 + \mathbf{p}_2\phi)^{\mathbf{p}_3}} \tag{14}$$

where p_1, p_2 and p_3 are the model parameters for each amino acid. The utilized model parameters p_1, p_2 and p_3 for tryptophan and phenylalanine were (11.6750, 11.980, 1.140) and (1.8817, 34.043, 0.623), respectively. It should be emphasized that the same Abel's model, with parameters for each amino acid, was utilized in the phi-plot design criteria (section 2) for the determination of the Henry's constants. After the acquiring of the mass transfer parameters (each ϕ value), linear interpolations in the modifier volume fraction domains for determination of the mass transfer parameter equations in the ϕ intervals were carried out. Eqs. 15 to 21 present the mass transfer parameter equations related to each ϕ interval, which were utilized in the proposed SG-SMB simulator. Such equations were applied in the calculations of the mass transfer parameters (according to ϕ values) utilized in the lumped mass transfer model of Eq. 13.

$$\eta_{1\ \text{phenyl}} = -602.89\ \phi + 335.75\ \left(0.0 \le \phi \le \phi_0\right) \tag{15}$$

$$\eta_{1\ \text{tryp}} = -7128.5\ \phi + 459.02\ \left(0.0 \le \phi < 0.05\right) \tag{16}$$

$$\eta_{1\ \text{tryp}} = 938.32\phi + 55.68\ \left(0.05 \le \phi < \phi_0\right) \tag{17}$$

$$\lambda_{2\ \text{phenyl}} = 2460.0\ \phi + 178.5\ \left(0.0 \le \phi < 0.05\right) \tag{18}$$

$$\lambda_{2\ \text{phenyl}} = 733.33\ \phi + 264.83\ \left(0.05 \le \phi \le \phi_0\right) \tag{19}$$

$$\lambda_{2\ \text{tryp}} = -486.0\ \phi + 39.3\ \left(0.0 \le \phi < 0.05\right) \tag{20}$$

$$\lambda_{2\ \text{tryp}} = 460.0\ \phi - 8.0\ \left(0.05 \le \phi \le \phi_0\right) \tag{21}$$

4.2. Phi-plot design criteria evaluation by SG-SMB simulator

The next Table 1 presents the two conditions (cases 1 and 2) studied by Nam et al. [1] in performance optimization of SG-SMB separations of phenylalanine and tryptophan. The

authors utilized distilled deionized water and ethanol as main solvent and modifier solvent. The adsorbent used was PVP resin (poly-4-vinylpyridine, cross linked) with intra-particle porosity of 0.55. The inter-particle porosity of the packed column was 0.33, obtained by tracer-molecule pulse tests. The conditions of Table 1 were utilized in the proposed design criteria approach, which was analyzed and evaluated through the new implemented SG-SMB simulator.

Zone flow rates (mL/min)	Case 1	Case 2
Q^{I}	10.00	10.00
Q^{II}	4.02	4.56
Q^{III}	9.06	11.21
Q^{IV}	3.62	4.52
Inlet/outlet flow rates (mL/min)		
Q_{feed}	5.04	6.65
Q_{des}	10.00	10.00
Q_{ext}	5.98	5.44
Q_{raf}	5.44	6.69
Switching time, t_{sw} (min)	25.95	21.97

Table 1. Optimized SG-SMB conditions studied by Nam et al. [1]

The two conditions of Table 1 were utilized in the phi-plot design criteria as well as in the SG-SMB simulator for three different values of porosity, the bed porosity (inter-particle), the intra-particle porosity and the total porosity, which correspond, respectively, to 0.33, 0.55 and 0.69. The last porosity value is the combination of both porosities, the inter-particle and the intra-particle. In the simulations carried out by Nam et al. [1] only the bed porosity and the intra-particle porosity were used in the robust modeling approach, respectively, in the mass transfer model of convection along the column combined with the mass transfer model inside the adsorbent pores. It should be noted that in the stepwise modeling approach applied in the present work only one porosity value is utilized in the model which is considered the total porosity. Therefore, any porosity value utilized in the present stepwise approach with lumped mass transfer model (SW-LM) is considered total porosity as such one assumes mass transfer phenomena in any kind of pore structure.

Table 2 presents the results of design criteria (χ equation) as well as of the SG-SMB simulator (purity values, productivity and solvent consumption) for three different values of total porosity, assuming the zone flow rates of case 1 in Table 1. As can be seen in Table 2, the best optimization result corresponds to that in which the χ equation tends to zero ($\chi \rightarrow 0$). This condition corresponds to the total porosity of 0.55, which is lower than the total porosity obtained by the bed porosity and the intra-particle porosity of PVP resin [1,23]. Such a porosity

http://dx.doi.org/10.5772/61252

value led to purities in the extract and raffinate higher than 99% with higher productivity and lower solvent consumption.

Porosity	0.33	0.55	0.69
χ	-1.63	0.67	3.83
Raffinate purity (%)	69.38	99.99	99.21
Extract purity (%)	100.00	99.45	73.87
Productivity (g/h.L)	0.431	0.580	0.474
Solvent consumption (L/g)	3.264	2.426	2.967

Table 2. Porosity effect in the SG-SMB performance

The SG-SMB simulation results of Fig. 5 show the concentrations of phenylalanine and tryptophan along the columns for the three different values of total porosity (0.33, 0.55 and 0.69). Moreover, it can be seen in Fig. 5 the ethanol (modifier) volume fraction along the chromatographic columns, which has a significant reduction in the concentration in the regions after the feed (F). In the simulation results, utilizing the porosity equal to 0.33 (Fig. 5A), it can be observed the contamination of the raffinate (R) with both substances leading to a lower purity value of phenylalanie in the raffinate (see Table 2). The contrary is observed utilizing the porosity of 0.69 (Fig. 5C) in which the contamination is situated in the extract (E), which reduces the purity of tryptophan in such a region (see Table 2). In the porosity value of 0.55 (Fig. 5B), there is only tryptophan in the extract (E) and phenylalanine in the raffinate (R) so the respective purity is higher in both regions.

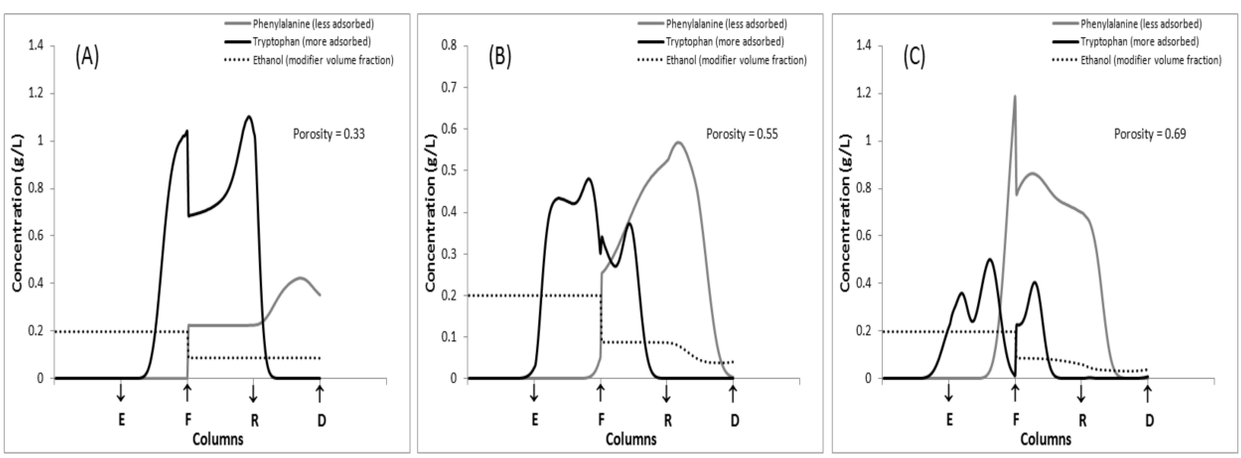

Figure 5. SG-SMB simulation results for the three studied values of total porosity

The design criteria results presented in Fig. 6 confirm the most favorable result for SG-SMB separation when utilizing the total porosity of 0.55 which led to the χ equation value of 0.63 (vide Table 2). The desirable inversion in the profiles (flow rate ratio–Henry difference) along

sections II and III can be noted in Fig. 6A. The phi-plot results of Fig. 6B (volume fraction of modifier (ϕ) versus flow rate–Henry difference) are in the positive region of the graph, which indicates the viability of complete separation for both molecules. The grey triangle and the black square, which represent the flow rate–Henry difference in sections II and III, respectively, are also in the positive region, which validates the inequalities of Eq. 8. The analysis in terms of sections II and III is important as such regions represent a key role in the separation performance of SMB process. The inequalities of Eqs. 1 to 4 are plotted in Fig. 6C as the difference in terms of flow rate ratio–Henry (m-H or H-m). As can be seen in Fig. 6C, all the m-H and H-m difference quantities are positive, which indicate that the inequalities of Eqs 1 to 4 are true for complete separation. The volume fraction of modifier (ϕ) along columns obtained utilizing the flow rate balance of Eq. 6 is plotted in Fig. 6D, which shows the significant reduction in ϕ concentration after the feed (F).

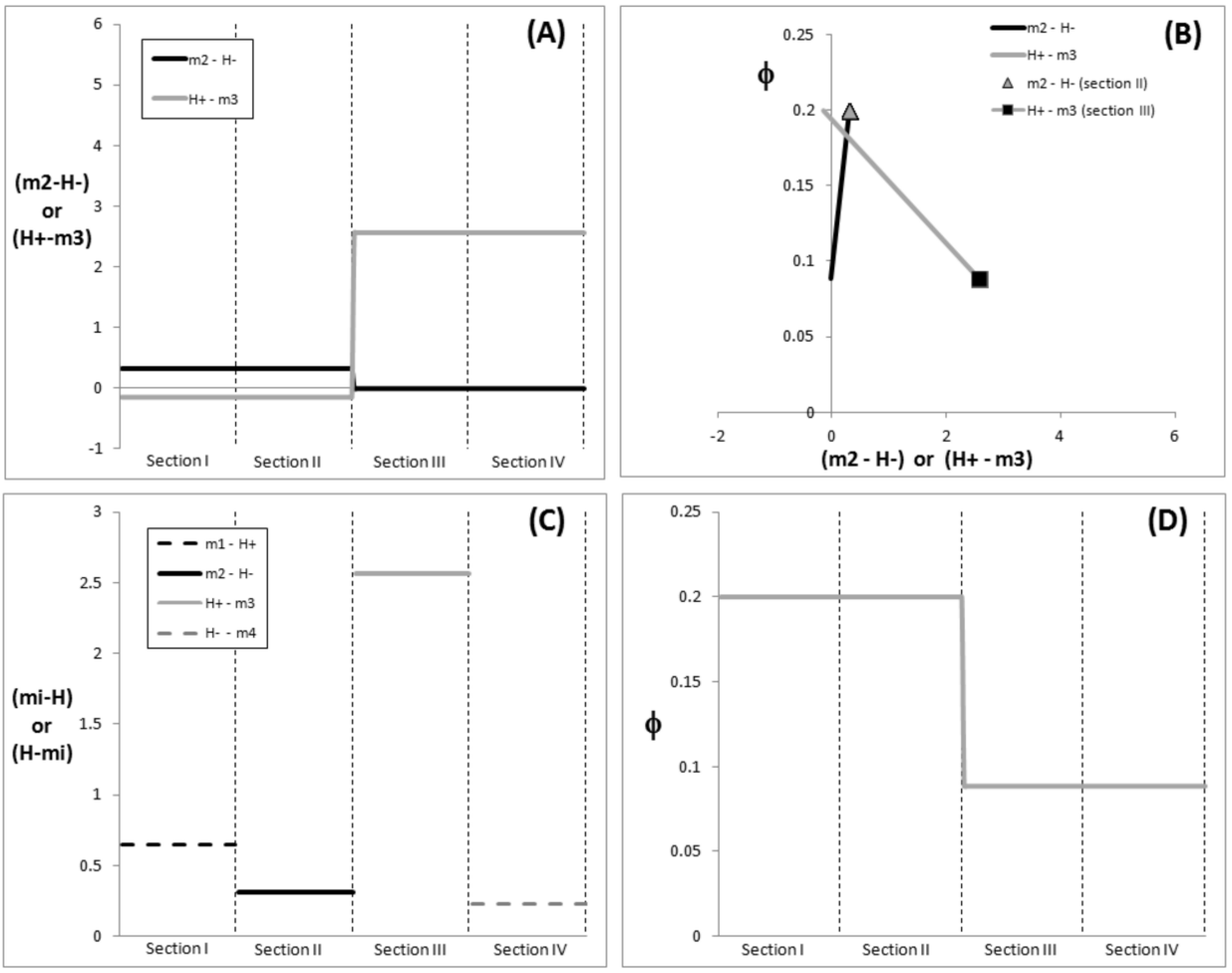

Figure 6. Design criteria approach with phi-plot results for total porosity of 0.55

Fig. 7 presents the design criteria results utilizing the ϕ distribution along the sections or columns (Fig. 7D) obtained not by the flow rate balance of Eq.6 but by the simulation results of the proposed SG-SMB simulator. Therefore, Fig. 6D and Fig. 7D were obtained, respectively,

http://dx.doi.org/10.5772/61252

via the flow rate balance of Eq.6 and the SG-SMB simulator. Comparing both Figs. 6D and 7D it can be seen that the profiles of ϕ are very similar differing only in section IV. So it can be noted that both design criteria results of Fig. 6 and 7 are very similar and have the same conclusions as the ϕ concentration profiles are almost the same. It should be realized that the modifier volume fraction (ϕ) is the main data utilized in the determination of all the design criteria results.

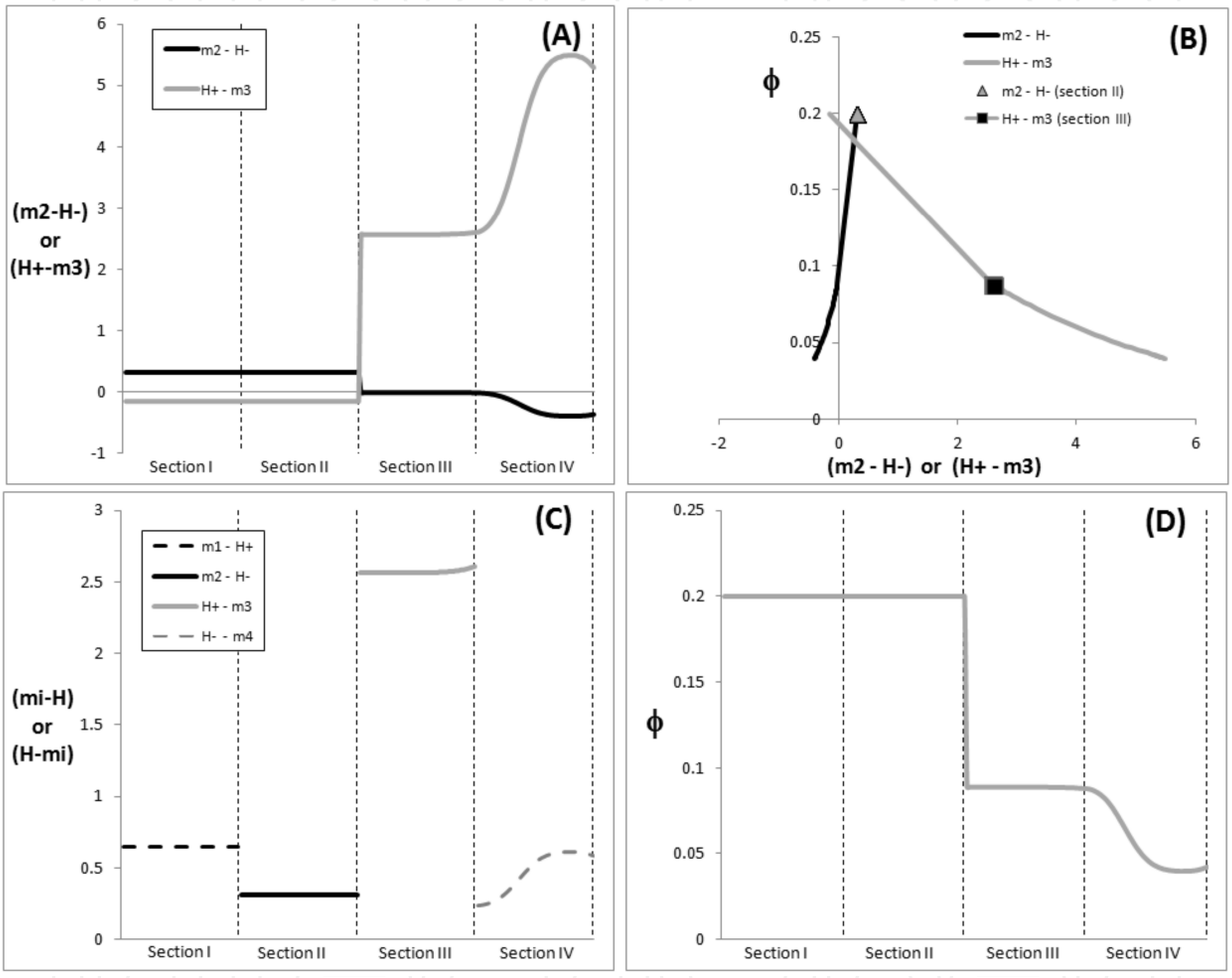

Figure 7. Design criteria approach with phi-plot results for total porosity of 0.55. The ϕ distribution obtained by SG-SMB simulator

Figs. 8 and 9 show the design criteria results for the two other porosity values in Table 2, 0.33, and 0.69, respectively. As can be seen in Table 2, the low porosity value of 0.33 led to a negative χ equation quantity (-1.63), which is far from the ideal ($\chi \rightarrow 0$) decreasing the purity in the raffinate. The low raffinate purity (see Fig. 5A) is due to the presence of both substances (phenylalanine and tryptophan) in raffinate (R) region after feed (F). Analyzing Fig. 8 it can be observed that the (H_+ - m_3) difference is not positive, so it is situated in the negative region of the phi-plot graph (Fig. 8B). The flow rate ratio in section 3 (m_3) is higher than the Henry constant as the (H_+ - m_3) difference is negative, therefore, the strong component (tryptophan)

is carried upwards, contaminating the raffinate. Such a conclusion is evident in Fig. 5A as the concentration profile of tryptophan (black line) is wider for right positions if compared to the profile of the best condition of complete separation (Fig. 5B). Another implication due to the negative difference of (H_+ - m_3) is the non-intersection of the profiles in Fig. 8A. In Fig. 8C it can be observed that the flow rate ratio in section IV (m_4) is higher than the Henry constant for the less adsorbed component ($H_{(-)}$-m_4<0) so less adsorbed molecules (phenylalanine) are carried upwards by the liquid phase, increasing its concentration in the upwards position as can be observed in section IV of Fig. 5A.

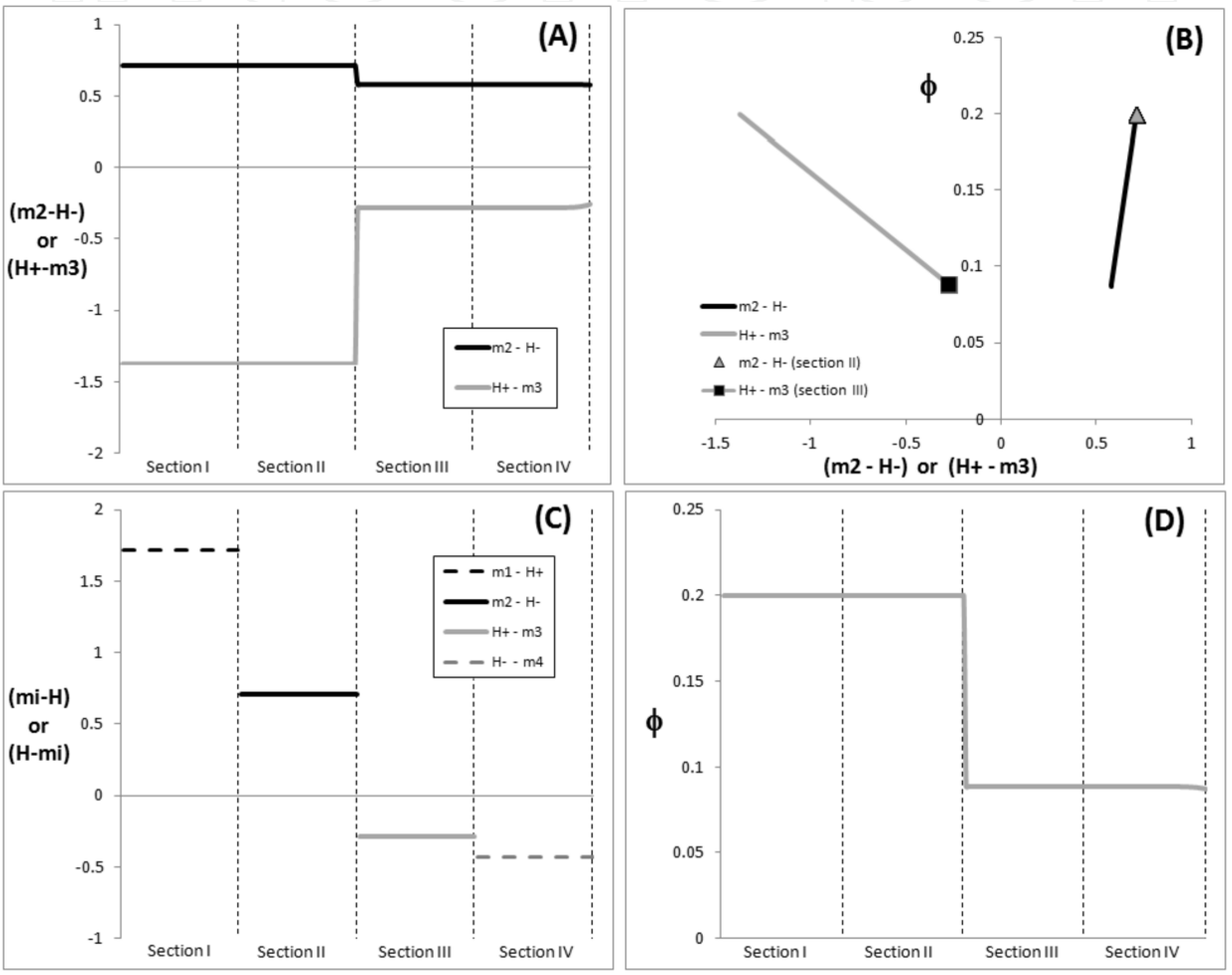

Figure 8. Design criteria approach with phi-plot results for total porosity of 0.33. The ϕ distribution obtained by SG-SMB simulator

The design criteria results for porosity equal to 0.69 are presented in Fig. 9 and it can be observed in the phi-plot of Fig. 9B that the (m_2-$H_{(-)}$) difference is negative so the Henry constant is higher than the flow rate ratio in section II. It means that the less adsorbed molecules (phenylalanine) are more retained in the solid adsorbent phase than it should be contaminating the extract port and reducing the purity. It is clear in Fig. 5C (porosity equal to 0.69) that the phenylalanine profile concentration (gray line) is wider (displaced to the left), reaching and

http://dx.doi.org/10.5772/61252

contaminating the extract port. As can be seen in Table 2, the high porosity value of 0.69 led to a positive χ equation quantity (3.83), which is far from the ideal ($\chi \rightarrow 0$), decreasing the purity in the extract. Moreover in section I, the Henry constant for the more adsorbed is higher than the flow rate ratio as the (m_1-$H_{(+)}$) difference is negative (Fig. 9C). So in section I the tryptophan is more retained by the solid adsorbent phase than it should be. The implication is a wider concentration profile (displaced to the left) of the more adsorbed molecules, which can be visualized in Fig. 5C for the tryptophan (black line). Fig. 9A shows that the ideal intersection profile is not achieved as the requirements for complete separation are not fulfilled.

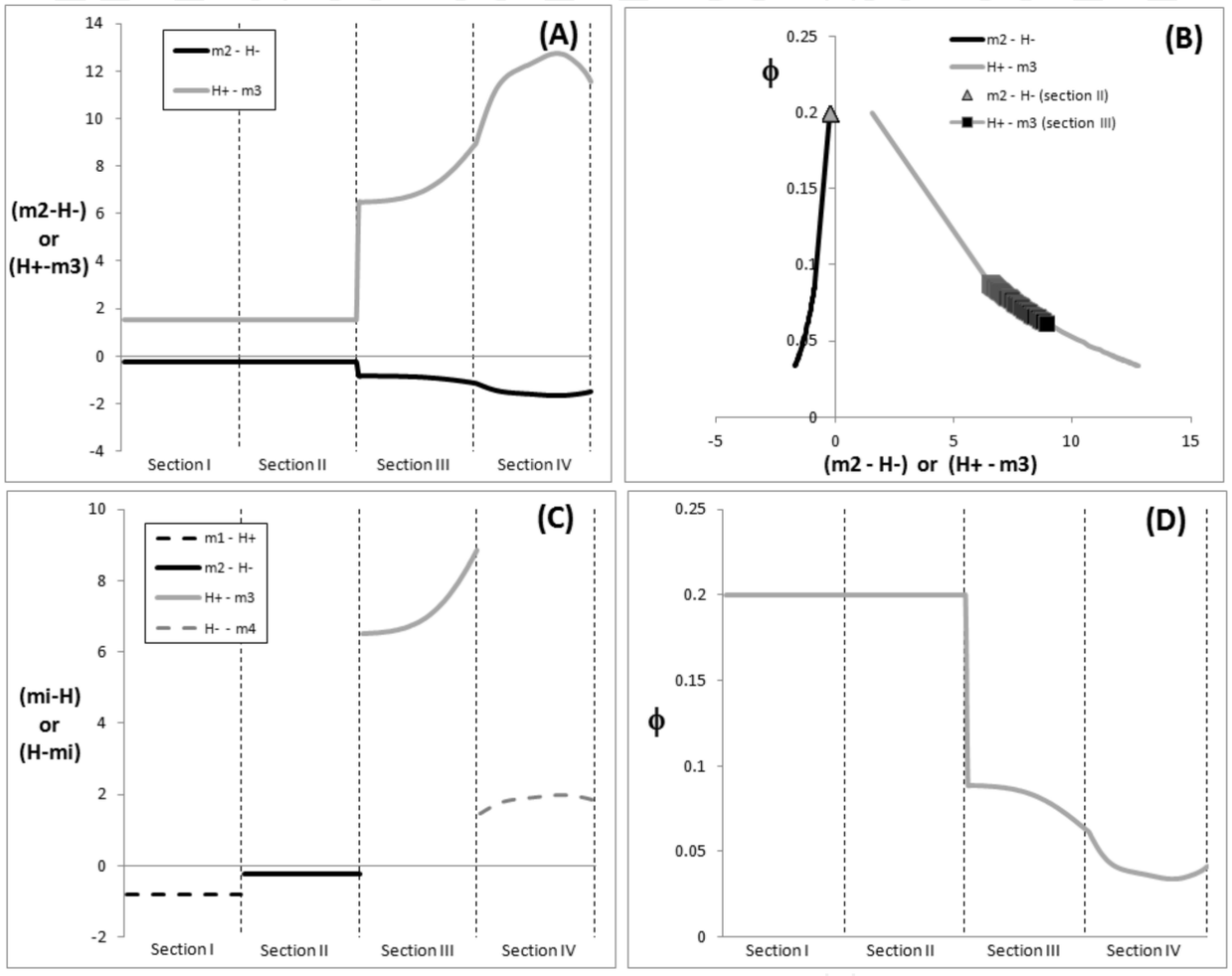

Figure 9. Design criteria approach with phi-plot results for total porosity of 0.69. The ϕ distribution obtained by SG-SMB simulator

The clockwise cyclic movement of the SG-SMB streams lead to cyclic concentration of molecules along time as can be seen in Fig. 10 for the two conditions of porosity, 0.55 (Fig. 10A) and 0.69 (Fig. 10B). Fig. 10 provides simulation results of concentration in the extract along time. In the condition of complete separation (Fig. 10A for porosity of 0.55), it can be observed the significant transient concentration of the more adsorbent molecule (tryptophan) if compared to the lower concentration of the less adsorbed (phenylalanine). The same separation

performance is not achieved in the porosity condition of 0.69 (Fig. 10B) as both molecules have significant values of concentration. The periodic concentration of molecules in Figs. 10A and B can be visualized, respectively, through the concentration profiles along the columns in Figs. 5B and C. In each switch time period, the extract port varies from the right, near the Feed (F), to a left position in which there is a variation in the concentrations with time that depends on the concentration profiles of each solute along the columns (vide Figs. 5B and C).

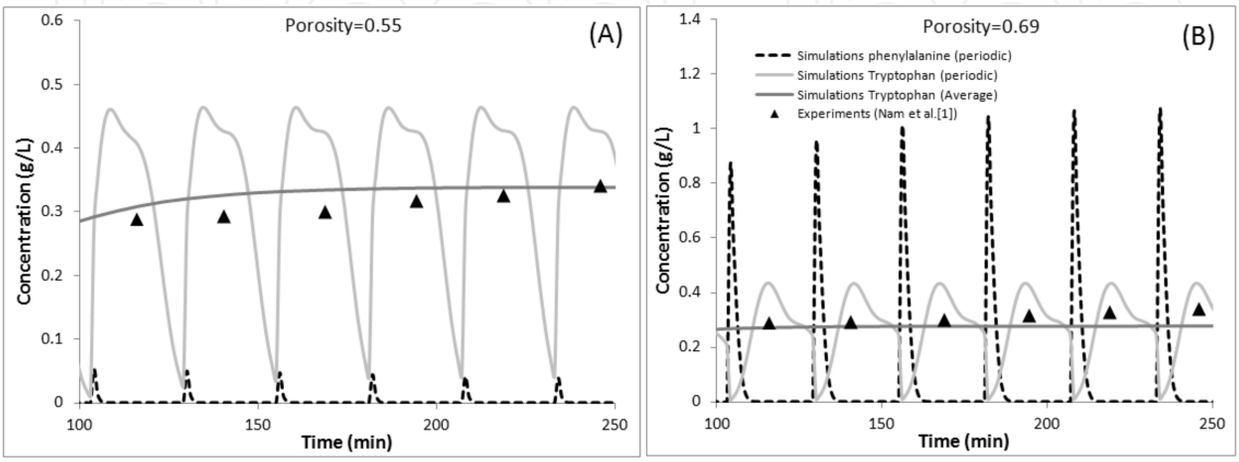

Figure 10. Concentrations along time in the extract of SG-SMB for porosity values of 0.55 (A) and of 0.69 (B)

Fig. 11 presents the correlations between the simulation results of the proposed SG-SMB simulator and the experimental data obtained by Nam et al. [1], who studied the separation performance of the amino acids phenylalanine and tryptophan in a SG-SMB unit. The simulations are plotted in terms of periodic (dotted lines) and average (solid line) concentrations along time in the extract as well as in the raffinate. From Fig. 11 it can be observed the good agreement between the average simulations and the experiments (black triangles) of Nam et al. [1] when utilizing the total porosity of 0.55. It must be remembered that there is no adjustment between the simulations and the experiments in Fig. 11 as it was utilized the mass transfer equations determined previously in the column characterization.

The two different operating conditions utilized by Nam et al. [1] and described in Table 1 were evaluated by the proposed SG-SMB simulator. The comparison results are presented in Table 3, and the close productivity values for both operating conditions studied can be seen. In terms of purity of extract and raffinate, the SG-SMB simulator provided values higher than those obtained by Nam et al. [1]. It can be observed that increasing the feed flow rate and reducing the switching time (second option) lead to a higher productivity with lower solvent consumption. The disadvantage in such a procedure is the reduction in both purities of the extract as well as raffinate.

New simulation results (SG-SMB simulator) for the optimization of productivity as well as solvent consumption were carried out increasing the feed flow rate as described in Table 4. In Table 4 it can be seen that it is possible to increase the productivity with solvent reduction by only adjusting the switching time. The purities had a small reduction, which was more evident

http://dx.doi.org/10.5772/61252

in the extract stream. Also in Table 4 there are the design criteria results in terms of χ equation. As described in Table 4, the feed flow rate increase led to optimization conditions far from the ideal as the χ goes far from zero.

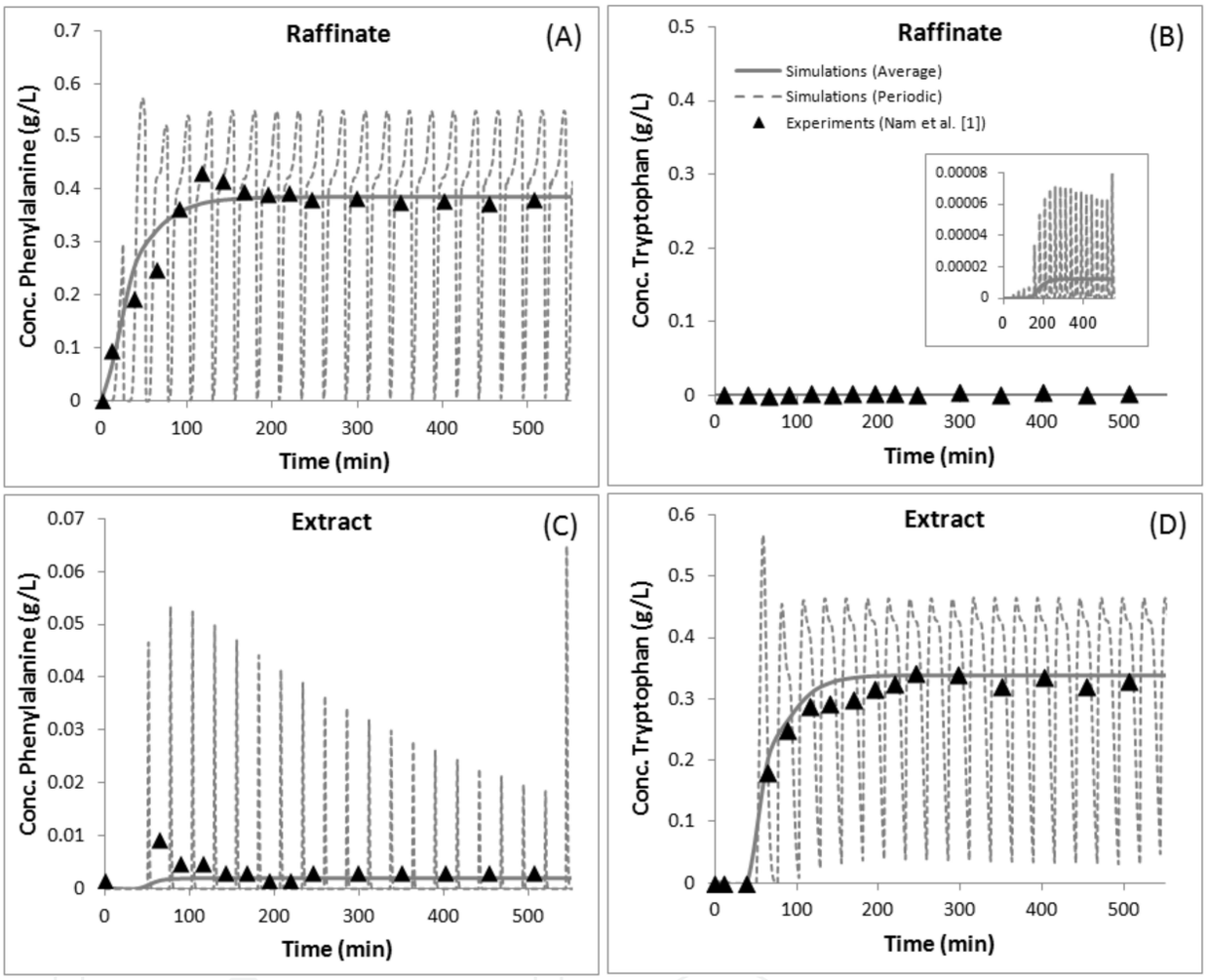

Figure 11. Comparisons between the simulation results from the SG-SMB simulator and the experimental data obtained by Nam et al. [1]; porosity equal to 0.55

	Nam et al.[1]	This work	Nam et al.[1]	This work
Feed flow rate (Q_{feed})	5.04	5.04	6.65	6.65
Switching time (min)	25.95	25.95	21.97	21.97
Raffinate purity (%)	98.00	99.99	97.40	99.85
Extract purity (%)	98.00	99.45	96.30	98.86
Productivity (g/h.L)	0.559	0.580	0.711	0.725
Solvent consumption (L/g)	-	2.426	-	1.943

Table 3. Separation performance of SG-SMB by comparison of two operating conditions

Feed flow rate (Q_{feed}) (mL/min)	5.04	10	15
Switching time (min)	25.95	28.00	25.00
χ	0.67	-2.36	-3.61
Raffinate purity (%)	99.99	99.91	99.91
Extract purity (%)	99.45	99.91	99.40
Productivity (g/h.L)	0.580	0.926	1.207
Solvent consumption (L/g)	2.426	1.522	1.167

Table 4. Improvement of productivity under feed flow rate increase (porosity equal to 0.55)

The phi-plot design criteria results related to feed flow rates of 10 and 15 mL/min (Table 4) are presented in Figs. 12A-B and 12C-D, respectively. According to Table 4 the χ equation values for feed flow rates of 10 and 15 mL/min were, respectively, equal to -2.36 and -3.61 so the higher feed flow rate corresponds to the inferior optimization condition (χ far from zero). In Fig. 12C such a conclusion is clear as the phi-plot of higher feed flow rate (15 mL/mi) is displaced to the left near the boundary of the positive region of the graph (compare Fig. 12A and C). Other results for the same feed flow rate (15 mL/min) show differences in the flow rate ratio–Henry (Fig. 12D) that are inferior in terms of domain if compared to those obtained using the feed flow rate of 10 mL/min (Fig. 12B). It should be emphasized that the optimization results from design criteria study are not a guarantee of complete separation of the molecules as the mass transfer effects of the real SG-SMB process are not assumed in such approach.

Different SG-SMB operating conditions were studied, comparing both the results of the SG-SMB simulator as well as of the design criteria approach. Table 5 presents the simulation results from the SG-SMB simulator as well as the design criteria approach studying four different operating conditions. As can be seen in Table 5, there is a strong relation between results of the design criteria and SG-SMB simulator as the last one confirmed the results obtained by the optimization approach. The design criteria results are in terms of separation performance in sections II (m_2 - $H_{(-)}$) and III ($H_{(+)}$ - m_3). In runs 1 and 2, such differences are positive, indicating complete separation of the molecules in the extract and raffinate. Such results are confirmed through the SG-SMB simulator that obtained simulation values of purities in the extract as well as in the raffinate higher than 99%. In run 3, the separation performance in section II (m_2 - $H_{(-)}$) is negative, indicating a contamination of the extract stream due to retention of the less adsorbed molecules (phenylalanine) on the solid adsorbent phase. This result is confirmed by the SG-SMB simulator, which presented a lower value of purity of the more adsorbed molecules (tryptophan) in the extract, which is equal to 65.03%. In run 4, the separation performance in section III ($H_{(+)}$ - m_3) is negative indicating a contamination of the raffinate stream due to convection transport of the more adsorbed molecules (tryptophan) by the liquid phase. This result is confirmed by the SG-SMB simulator, which presented a lower value of purity of the less adsorbed molecules (phenylalanine) in the raffinate, which is equal to 59.40%.

http://dx.doi.org/10.5772/61252

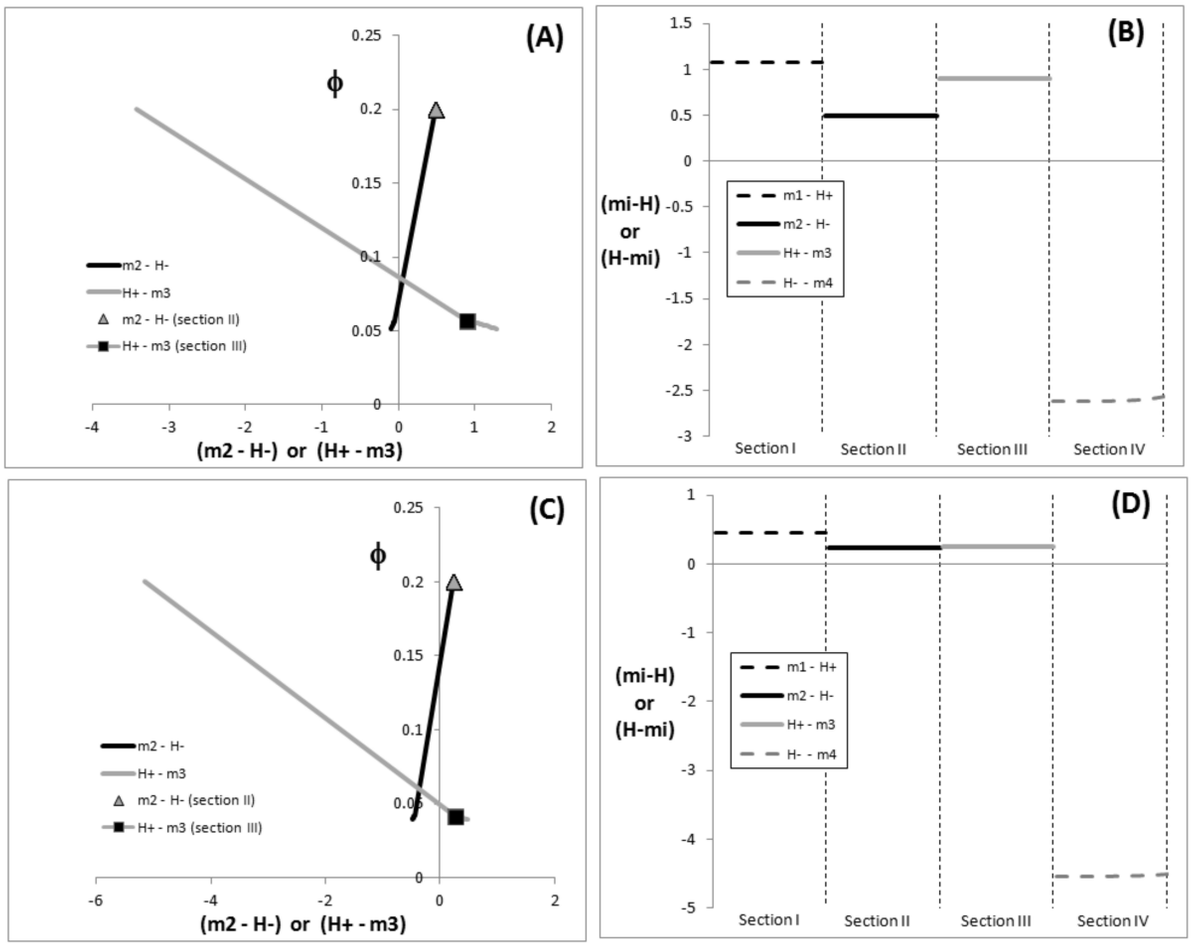

Figure 12. Phi-plot design criteria for feed flow rate of 10 mL/min (A and B) and 15 mL/min (C and D) related to simulation results in Table 4

	Run 1	Run 2	Run 3	Run 4
Q^{I} (mL/min)	15.0	7.0	7.0	12.0
Q^{II} (mL/min)	10.0	5.0	2.0	6.56
Q^{III} (mL/min)	20.0	8.0	12.0	18.56
Q^{IV} (mL/min)	15.0	6.0	7.0	11.87
Switching time (min)	15.5	34.5	37.0	25.0
porosity	0.7	0.7	0.7	0.55
m_2 - $H_{(-)}$	1.297	1.844	-1.238	1.560
$H_{(+)}$ - m_3	3.732	3.292	7.012	-2.206
Raffinate purity (%)	99.85	99.87	99.84	59.40
Extract purity (%)	99.98	99.99	65.03	99.99
Productivity (g/h.L)	0.599	0.185	0.747	0.802
Solvent consumption (L/g)	3.523	5.326	1.319	2.108

Table 5. Separation performance of SG-SMB for several conditions (ϕ=0.2)

5. Conclusions

The new design approach, which is based on equilibrium theory and utilizes the χ equation and phi-plot analysis, was able to predict a great number of operating conditions for complete separation in the solvent gradient simulated moving bed (SG-SMB) process. Optimal results were validated by the simulations carried out by the new implemented SG-SMB simulator, which is based on a stepwise approach combined with a lumped mass transfer model (SW-LM). The influence of the solvent modifier was considered, applying the Abel model which takes into account the effect of modifier volume fraction over the partition coefficient. The optimal conditions determined from the new design approach were compared to the simulation results of a SG-SMB unit applied to the experimental separation of the amino acids phenylalanine and tryptophan. Such a SG-SMB simulator provided simulation results with very good agreement fitting the experimental data of the amino acids concentrations both in the extract as well as in the raffinate.

Acknowledgements

The author thanks UERJ, Faperj, CNPq, and Capes for the financial support.

Author details

Leôncio Diógenes Tavares Câmara

Address all correspondence to: dcamara@iprj.uerj.br; diogenescamara@gmail.com

Dep. Mechanical Eng. and Energy – DEMEC, Polytechnic Institute of the State University of Rio de Janeiro (IPRJ-UERJ), Nova Friburgo, Brazil

References

[1] H.-G. Nam, S.-H. Jo, C. Park, S. Mun, Experimental validation of the solvent-gradient simulated moving bed process for optimal separation of phenylalanine and tryptophan, Process Biochem. 47 (2012) 401-409.

[2] S. Mun and H.-H. L. Wang, Optimization of productivity in solvent gradient simulated moving bed for paclitaxel purification, Process Biochem. 43 (2008) 1407-1418.

[3] G. Ziomek, D. Antos, Stochastic optimization of simulated moving bed process sensitivity analysis for isocratic and gradient operation, Comput. Chem. Eng. 29 (2005) 1577-1589.

[4] G. Ziomek, M. Kaspereit, J. Jezowski, A. Seidel-Morgenstern, D. Antos, Effect of mobile phase composition on the SMB processes efficiency stochastic optimization of isocratic and gradient operation, J. Chromat. 1070 (2005) 111-124.

[5] D. Antos, A. Seidel-Morgenstern, Application of gradients in the simulated moving bed process, Chem. Eng. Sci. 56 (2001) 6667-6682.

[6] D. Antos, A. Seidel-Morgenstern, Two-step solvent gradient in simulated moving bed chromatography-Numerical study for linear equilibria, J. Chromat. A. 944 (2002) 77-91.

[7] S. Abel, M. Mazzotti, M. Morbidelli, Solvent gradient operation of simulated moving beds- I. Linear isotherms, J. Chromat. A. 944 (2002) 23-39.

[8] S. Abel, M. Mazzotti, M. Morbidelli, Solvent gradient operation of simulated moving beds- 2. Langmuir isotherms, J. Chromat. A. 1026 (2004) 47-55.

[9] L. D. T. Câmara, Optimization strategies in the modelling of SG-SMB applied to separation of phenylalanine and tryptophan, J. Phys.: Conf. Ser. 490 (2014) 012033.

[10] F. Wei, B. Shen, M. Chen, Y. Zhao, Study on a pseudo-simulated moving bed with solvent gradient for ternary separations, J. Chromat. A. 1225 (2012) 99-106.

[11] J.-G. Lu, Y.-X. Sun, Mathematical modelling of non-linear solvent-gradient simulated moving bed chromatographic separation processes, Dev. Chem. Eng. Mineral Process. 13/1-2 (2005) 193-202.

[12] N. V. D. Long, J. W. Lee, T.-H. Le, J.-I. Kim, Y.-M. Koo, Solvent-gradient SMB to separate o-xylene and p-xylene, Korean J. Chem. Eng. 28/4 (2011) 1110-1119.

[13] D. Antos, A. Seidel-Morgenstern, Application of gradients in the simulated moving bed process, Chem. Eng. Sci. 56 (2001) 6667-6682.

[14] M. Nagy, T. Szánya, Z. Molnár, G. Turza, G. Gál, L. Hanák, J. Argyelán, A. Aranyi, K. Temesvári, Z. Horváth, Separation of organic compounds by gradient simulated moving bed chromatography, Hung. J. Ind. Chem. 34 (2006) 21-26.

[15] W. Klaus, S. Arthur, S.-T. Henner, Modelling and validated simulation of solvent-gradient simulated moving bed (SG-SMB) processes for protein separation, in: L. Puigjaner (Ed.), ESCAPE - 15, Barcelona, 2005, pp. 313-304

[16] C. Migliorini, M. Wendlinger, M. Mazzotti, M. Morbidelli, Temperature gradient operation of a simulated moving bed unit, Ind. Eng. Chem. Res. 40 (2001) 2606-2617.

[17] D. A. Horneman, M. Ottens, J. T. F. Keurentjes, L. A. M. van der Wielen, Micellar gradients in size-exclusion simulated moving bed chromatography, J. Chromat. A. 1113 (2006) 130-139.

[18] J. Houwing, H. A. H. Billiet, L. A. M. van der Wielen, Optimization of azeotropic protein separations in gradient and isocratic ion-exchange simulated moving bed chromatography, j. Chromat. A. 944 (2002) 189-201.

[19] M. Mazzotti, G. Storti, M. Morbidelli, Supercritical fluid simulated moving bed chromatography, J. Chromat. A. 786 (1997) 309-320.

[20] B. M. Thome, C. F. Ivory, Continuous voltage gradients and their application to true moving bed electrophoresis, J. Chromat. A. 1129 (2006) 119-128.

[21] L. D. T. Câmara, Stepwise model evalution in simulated moving-bed separation of ketamine, Chem. Eng. Technol. 37/2 (2014) 301-309.

[22] H.-G. Nam, T.-H. Kim, S. Mun, Effect of ethanol content on adsorption equilibria of some useful amino acids in poly-4-vinylpyridine chromatography, J. Chem. Eng. Data. 55 (2010) 3327-3333.